Available online at www.sciencedirect.com

ScienceDirect

journal homepage: www.elsevier.com/locate/he

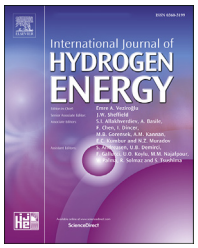

High-temperature green hydrogen production: A innovative– application of SOEC coupled with AEC through sCO_2 HP

Gianluigi Lo Basso, Ali Mojtahed, Lorenzo Mario Pastore, Livio De Santoli*

Department of Astronautical, Electrical and Energy Engineering, University of Sapienza of Rome, Rome, Italy

HIGHLIGHTS

- Green hydrogen production.
- Coupling layouts between low and high-temp water electrolysis.
- Featuring a cutting-edge technology of supercritical CO_2 HP for heat recovery.
- Improving total energy efficiency through coupling layout compared.
- Lower LCOH in coupling configuration compared with SOEC.

ARTICLE INFO

Article history:
Received 15 December 2022
Received in revised form
4 March 2023
Accepted 20 April 2023
Available online 11 May 2023

Keywords:
Green hydrogen
sCO_2HP
High -temp electrolysis
Energy efficiency
LCOH
Heat recovery

ABSTRACT

This study evaluates a potential coupling between AEC and SOEC through a CO_2 heat pump unit that works in super-critical conditions. In such a way, thermal power requested by SOEC can be provided by recovering heat loss from AEC via the CO_2heat pump. The coupled configuration is characterized by renewable electric input. Hence, the power is provided for electrolysis without more external thermal resources. The energy, economic and environmental impacts of such intervention have been determined and compared with SOEC in solo mode. The layout is created and simulated in a MATLAB SIMULINK environment.

The simulation results show a potential improvement in the total energy efficiency of the whole system without an external heat resource, up to 68%, which is higher than 65% of SOEC itself, thanks to the heat recovery section that is correlated with sCO_2 HP contribution. LCOH varies widely depending on SOEC size from around 2.59 €/kg_{H2} up to 9.27€/kg_{H2}.

Introduction

The tendency to shift from fossil fuels toward sustainable solutions has started to accelerate in recent years. A proper energy carrier candidate in addition to sustainability should be promising in both energy and economic aspects. Hydrogen is a leading energy career which carries the label of "future fuel" for couple of decades [1]. Its thermophysical properties make it a good energy solution to replace existing system. Furthermore, hydrogen likewise fossil fuels can be considered multi-functional by being implemented into various applications. In

* *Corresponding author.*
E-mail address: Ali.mojtahed@uniroma1.it (A. Mojtahed).
https://doi.org/10.1016/j.ijhydene.2023.04.231

transportation, heating purposes via burning or even in power generation in gas turbine systems [2–4]. Adding to them, hydrogen can be produced totally from renewable resources with zero carbon footprint. In this case, the outcome is known as "green hydrogen" [4]. As of today, the main renewable resources to produce hydrogen can be categorized into biomass process and water-splitting technologies using solar or wind power [5]. Thermochemical methods and biological ones are two well-recognized way to produce H_2 from biomass [6]. Through thermochemical process, hydrogen of hydrogen enrich gas is produced. They are mostly involved with pyrolysis or gasification methods. In order to increase the production ratio, water gas shift (WGS) reaction and/or various reforming techniques are integrated to the main process [7–9].

Water has merits of no pollutant emissions such as SO_x, CO_2 and CO, very simple working principle and being available all around the world [10]. Despite the fact that water electrolysis has been around for almost two century [11], there are a few mature technology available as of today. Proton exchange membrane (PEM) and Alkaline electrolysis Cell (AEC), are two commercial types of water electrolysis which both are categorized as low temperature electrolysis (LTE) [12]. LTE systems are characterized with nearly ambient operating temperature (up to 90 °C). Despite their technological superiority, still there are some demerits dealing with LTE specially alkaline ones such as: low partial load range, high ohmic loss and low current density [13,14]. The electric efficiency at its best is 70% based on LHV_{H2} but mostly in the range of 56–63 °CS. Some research works, have tried to improve the performance of LTE [15]. For instance Ref. [16], achieved lower cell voltage of water splitting in AEC via presenting a heterojunction hybrid structure of MoS_2@$Ni_{0.96}S$. For PEM electrolysers, several works attempt to increase the electrochemical performance. As an example [17], reported significant current density increase by developing a platinum free cobalt phosphide (Co–P) electrode for the hydrogen revolution reaction. Such an electrode is carbon fabricated by pulse electrodeposition technique using different dissolution of Co. High temperature electrolysis (HTE) in the other hand, consumes less electricity and promises the higher electric efficiency [18]. Some research works indicated the efficiency of hydrogen to water conversion above 100% through HTE is achievable [14,19]. The operating temperature is in the range of 600–950 °C which hails more thermodynamic and electrochemical kinetic advantages [20]. Nevertheless, it is characterized with an additional thermal consumption. One well-known high-temp technology is Solid oxide electrolysis cell (SOEC) which is still in R&D stage. The main drawbacks of SOEC that constrain further development is high specific cost and lower lifetime comparing with LTE [21–23]. Table 1 summarizes the main properties of water electrolysis technologies.

Having mentioned main characteristics of HTE, the current work aims to justify the application of SOEC that offers a feasible solution. A novel configuration containing both HTE and LTE operating in coupling mode attempt to address the main demerits of SOEC which are an additional heat resource and the cost effectiveness. To do so, a cutting edge technology supercritical CO_2 heat pump is employed for heat recovery inside the plant. The role of this component is to provide the thermal requirement for SOEC without the necessity of an external source. The case study is supplied 100% from renewable generation leading to green hydrogen production with promising environmental benefits. In addition to that, the energy performance of such system is simulate via MATLAB SIMULINK. A comprehensive economic analysis is carried out to evaluate the final cost of hydrogen production which is expressed in terms of levelized cost of hydrogen (LCOH) and carbon avoidance cost.

The main missions of this work can be concluded as follow:

Introducing the coupling layout between LTE and THE.

Improving energy efficiency by implementing heat recovery through sCO_2 HP.

Describing useful energy performance of sCO_2 Heat pump.

Final H_2 production from only renewable generation.

Techno-economic comparison between coupling layout and conventional SOEC application.

Environmental impacts assessment.

CO_2 in the literature

CO_2 is one of the first natural refrigerants that has been in use for many decades. Its thermophysical properties make it a good choice for undergoing a thermodynamic cycle. As concerns of the heat pump systems, the role of CO_2 in trans critical cycle has been already defined to produce domestic hot water [36] and cooling effect [37]. In a trans critical cycle, the refrigerant goes over the critical conditions only on the upstream side of the cycle. In super critical cycle however, the refrigerant remains in gaseous phase all over the process causing no phase change at all [38]. Super critical CO_2 has many applications in industry specially power cycles. In nuclear engineering, sCO_2 Bryton cycle is used for power conversion to increase the efficiency of generation IV reactors due to its capacity to provide higher turbine outlet temperature in comparison with steam Rankine cycle [39]. Except for nuclear application, sCO_2 power cycle can be used as a topping cycle for fossil fuel powered plants and a bottoming cycle of gas combined cycle plants [40], or for exhaust/waste heat recovery application [41]. The thermodynamic properties of sCO_2 creates new opportunities in turbomachinery designs. High pressure and densities result in compact component designs which eventually reduces the size of the machine and the cost. Decreasing the diameter of turbomachinery however, induces a new line of problems associated with high rotating speed. As an example, increased tip-clearance and secondary-flow losses, challenges in the design of the shaft, bearings and seals to ensure stable rotor dynamic behaviour across the range of expected operating speeds, are some major problems related to increasing aerodynamic losses [42]. As discussed in literature [43–45], sCO_2 cycle can also be defined to improve the economic indicators in renewable resources by recovering the waste heat specially for fuel cells applications. Another usage of sCO_2 in the field of renewable generation is defined inside solar concentration systems. As an example, in Ref. [46], sCO_2 is presented in U shaped double piped heat exchanger structure to concentrate solar power. The numerical results suggest the temperature increase of sCO_2 as a more effective parameter to improve the conventional heat transfer coefficient rather than pressure.

Having discussed the current applications available for sCO_2 cycle, a new line of operation can be added to the list by

Table 1 – Main characteristic of available water electrolysis cells.

Electrolyte	Alkaline	PEM	SOEC
	20–30% KOH	PFSA	YSZ
Current density (A cm^{-2})	0.2–0.4	0.6–2.0	0.5–1.5
Cell voltage (V)	1.8–2.4	1.8–2.2	0.9–1.5
Electrical efficiency (%LHV)	63–70	56–60	74–81
Temperature range (°C)	65–100	70–90	650–1000
Discharge pressure (bar)	25–30	30–80	1–10
Stack Lifetime (h)	30 000–90 000	60 000–90 000	10 000–30 000
H_2 Purity (%)	99.3–99.9	99.9999	99.99
Specific energy consumption (kWh Nm^{-3})	4.8	5.2	3.6
Capacity (Nm^3h^{-1})	1–760	0.265–30	87
Specific cost (€/kW_e)	450–1270	590–1360	2500–5000
Degradation rate (%voltage increase in kh)	0.011	0.14	0.9
Technology maturity	Mature	Mature for small scale	R&D
Reference	[5,19–22,24]	[10,14,25,28–31]	[23,27,32–35]

implementing sCO_2 in a heat pump [47]. This potential configuration is integrated with water electrolysis in low-temp and high-temp region coupling them in such a way that the waste heat from LTE is recovered and imported to the HTE. Fig. 1, demonstrates the P-h diagram of sCO_2 thermodynamic cycle inside the heat pump. Assuming CO_2 critical point at 31 °C, 73 bar, due to the criteria in down and upstream side of the cycle, the refrigerant remains at super critical state all over the loop. The detailed structure of HP unit is explained at methodology section.

Methodology

Fig. 2 a and b, illustrates the schematic of the proposed layout. Instead of an external heat resource to generate the steam required for SOEC, sCO_2 HP unit is implemented for heat recovery. The energy losses during the electrolysis process is correlated with joule effect inside AEC. The contribution of sCO_2 HP is to recover AEC thermal losses by elevating fluid temperature sufficient enough for high-temp application. The operating temperature inside SOEC stack is in range of 600–950 °C. The stack can operates in three different mode that strictly correlated with input temperature and applied current: endothermic, exothermic and neutral thermal [48]. Based on the electric efficiency of the stack, during the electrolysis process part of the electric power will be lost in form of heat, increasing the temperature of the stack. When the heat caused by electric power exceeds the heat required for electrolysis reaction, the stack operates in exothermic conditions rising in-stack temperature. In endothermic conditions, provided heat cannot respond to the demand for the reaction so additional external heat should be delivered to the stack. As a result, in endothermic mode, in addition to electric power, a heat source should be implemented for completing the electrolysis reaction. Such heat should provide only a portion of

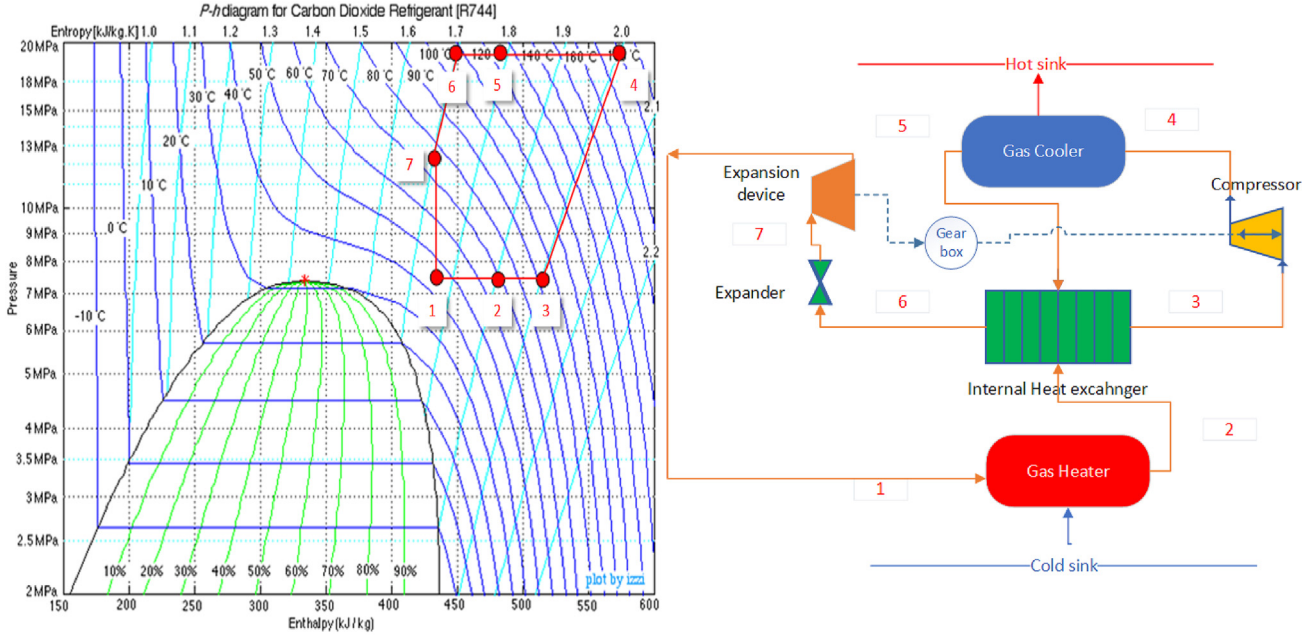

Fig. 1 – P-h diagram of CO_2 operating in super critical state.

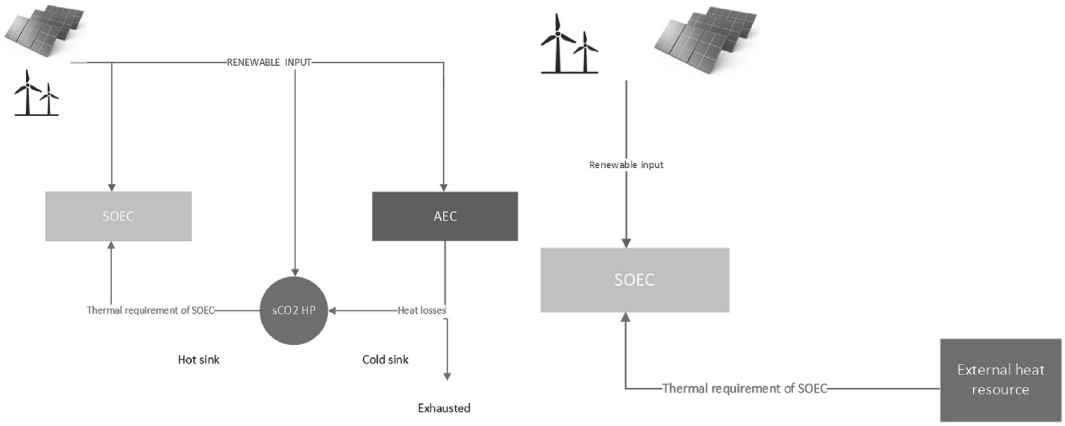

Fig. 2 – a) the coupling configuration including AEC and SOEC which are linked together through sCO_2 HP b)SOEC configuration in solo-mode integrated with an external heat resource to meet the thermal requirement.

the total heat that is missing. Based on the commercial models available, required thermal energy is reported in terms of input steam profile which should be delivered to the stack. Based on chosen model the thermal input profile is characterized with the steam in 150 °C and 3.5 bar. Table 2, shows the steam requirement of the commercial SOEC model which is assumed for simulation [32,49]. The heat pump role is to deliver sufficient heat to generate steam to meet the SOEC starting operation set point. Thermophysical properties of CO_2, has been considered to size properly the heat pump. AEC stack that is assumed as cold sink of the HP, ensures the thermodynamic cycle to be held totally above critical point and avoiding the phase change. The expansion process is consist of two phases as illustrated in Fig. 3. Due to the extreme fall down undergoing isentropic expansion through expander, the refrigerant drops below critical point. In order to avoid such effect, a mid-pressure is defined down to the point that ensures super critical condition. Afterward, the refrigerant undergoes an additional isenthalpic expansion through an expansion valve. In this way, it is possible to benefit some amount of mechanical work from isentropic expansion and spend it for compression process. With an external steam generator fed with natural gas and the same power income from renewable is taken into account.

Simulation

In the hybrid layout, the generated power is divided into three sections. In this way, the size of SOEC and AEC is correlated with each other. SOEC sizing can be characterized by changing the vapor flow rate. Subsequently, the thermal load of sCO_2 HP can be sized. The remaining part of the power is dedicated to AEC. Since commercial alkaline electrolysers are available in a wide range of capacity, different commercial models can be chosen in this part. Eq. (1):6, explain the working principle of simulation part. In there, $\dot{m}$ is the steam flow rate which is characterized with SOEC input criteria.

$$P'_{RES} = P'_{el\_SOEC} + P'_{sCO2HP} + P'_{AEC} + P'_{l} \quad (1)$$

$$P'_{th\_SOEC} = \dot{m}\, C\, (T_{sat} - T_w) + \dot{m}(h_{sv} - h_{sl}) + \dot{m}(\, h_{dp} - h_{sv})\, P'_{th_{SOEC}} \quad (2)$$

$$P'_{th\_SOEC} = Q_{H\_HP} \quad (3)$$

$$Q_{d\_AEC} \geq Q_{C\_HP} \quad (4)$$

$$W_{HP} = Q_{H\_HP} - Q_{C\_HP} \quad (5)$$

$$P'_{AEC} = P'_{RES} - P'_{el\_SOEC} - W_{HP} - P'_{l} \quad (6)$$

Solar and wind renewable resources have been assumed for power generation. Since the renewable income is not programmable and changes instantaneously, the equivalent peak hour for solar and wind in region of Italy, city of Rome, has been assumed instead of going through hourly simulation. Such an assumption has been made generally for the sake of simulation. It is not intended to assess an accurate dynamic model since such a parameter is not an effective indicators for the system. Of course such a model can be adapted for various climate profiles which could be the scope of future works. In this way, by assuming a fixed available energy during the year for both layouts, the energy efficiency and hydrogen production rate can be compared with each other. In Ref. [50], the equivalent hours for renewable sources for Italy is illustrated. The detailed report about solar radiation hours for the city of Rome can be found in Ref. [51]. In average an equivalent hours equal to 1425 and 1732 h per year has been considered for PV and wind generation respectively. The peak power at is set at 500 kW. This value is selected based on one of the available commercial SOEC size which is equal to 160 kW in order to ensure at least 3000 equivalent hours for the operation. In section "result and discussion", the sensitivity analysis for various sizes is performed to study the impact of such parameter on H_2 cost reduction.

Table 2 – Steam profile of the SOEC.

Temperature (°C)	150 …. 200
Pressure (Bar)	3.5 …. 5.5
Steam to H_2 ratio (kg_{steam}/Nm^3_{H2})	0.74
Nominal Power (kW)	65, 160, 250, 350

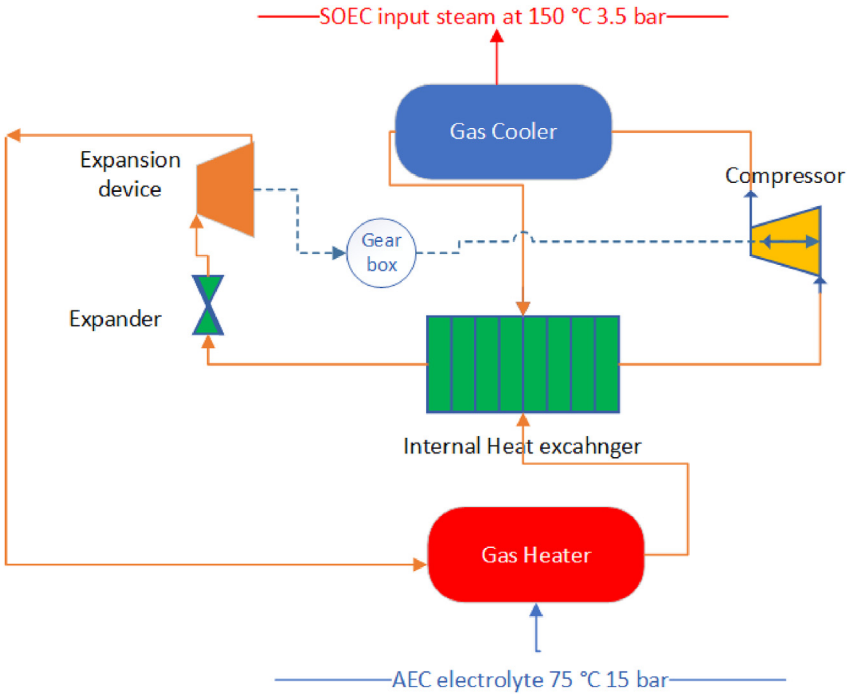

Fig. 3 – The working principle of sCO_2 HP in coupling configuration integrated with AEC and SOEC.

Table 3, shows the main assumptions have been used for simulation. An optional value of 500 kW is considered for renewable power input. The final results would be normalized by input power. Hence, the input could be any other value and does not affect the energy performance of the system. For electrolysers part, except for the efficiency, the degradation value has been reported which affects the H_2 production during the lifetime. The simulation part, has been carried out inside MATLAB SIMULINK environment.

Economic assumption

Economic assumption–Environmental impact introduce useful indicators to analyse the simulation results. Such formulas subsequently are employed in Result and Discussion.

Economic assessment is expressed by deriving the levelized cost of hydrogen (LCOH) which is an effective indicator to indicate the total investment cost per each kg of production [26,52,53]. LCOH can be defined by eq. (7):

$$LCOH = \frac{crf \cdot CAPEX + C_{O\&M,y}}{m_{H2,y}} \quad (7)$$

where:

$m_{H2,y}$ is the annual hydrogen production by mass,

$C_{O\&M,y}$ are the annual costs for operation and maintenance

$CAPEX$ is the Capital Expenditure

crf is the capital recovery factor, which can be calculated according to (eq (8)).

$$crf = \frac{i \cdot (1+i)^{\tau}}{(1+i)^{\tau} - 1} \quad (8)$$

In which i is the discount rate and τ is the lifetime of the project

The economic assumptions have been reported in Table 4. For renewable generation, the levelized cost of electricity for Italy in 2020 has been considered [54].

For sCO_2 HP capex estimation, is performed due to the lack of practical data and the fact that such technology has been defined for the first time in the literature. Nevertheless, the

Table 3 – List of technical assumptions for simulation part.

	Value	Unit
SOEC efficiency	77%	–
SOEC degradation rate	0.9	% of voltage increase in kh
SOEC steam to H2 ratio	0.87	Nm^3_{H2}/kg_{steam}
SOEC steam input temperature	150	°C
SOEC steam input pressure	3.5	Bar
AEC efficiency	58%	–
AEC degradation rate	0.011	% of voltage increase in kh
AEC stack temperature	75	°C
PV equivalent hours	1263	h/year
Wind equivalent hours	1732	h/year
Heat exchanger effectiveness	0.7	–
Isentropic efficiency	0.78	–

Table 4 – The list of economic assumptions.

	Unit	Specific capital cost	O&M (€/kW)	Lifetime	Ref
SOEC	€/kW_e	3000	80	10 000–30 000 h	[55]
AEC	€/kW_e	950	19	60 000–90 000 h	[55]
PV	€/kWh	0.088	10	20 y	[54]
Wind	€/kWh	0.083	70	25 y	[54]
NG	€/kWh	0.117	–	–	[56]

Table 5 – sCO_2 simulation results.

Steam flow rate (kg_{steam}/h)	Hot sink size (kW)	Cold sink size (kW)	Available heat for recovery (kW)	η_{th}	SOEC size (kW)	AEC size (kW)
20	18.15	6.99	181	3.8%	62.64	431.8
50	45.37	17.48	138.7	12.6%	156.6	329.5
75	68.06	26.22	102	25.7%	234.9	244.2
110	99.82	38.46	52.45	73.3%	344.5	124.8

experimental model that has been introduced [57] for trans critical CO_2 HP has been considered as the reference.

Energy efficiency

One of the main privileges of coupled hybrid configuration is its impact on total energy efficiency of the system. The energy efficiency (EE) can be defined as the effective energy spent for H_2 production vs the total energy imported to the system:

$$EE = \frac{E_{H2}}{E_{tot}} \tag{9}$$

where E_{tot} is the total energy that is consumed by the system.

In coupled scenarios, the only input is the renewable resource generation. However, in SOEC solo mode, in addition to renewable income, there is a natural gas consumption for thermal load. As a result eq.9 can be rewritten for each case:

$$EE_{coupled} = \frac{LHV_{H2} * m_{H2}}{E_{RES}} \tag{10}$$

$$EE_{SOEC-solo} = \frac{LHV_{H2} * m_{H2}}{E_{RES} + LHV_{NG} * m_{NG}} \tag{11}$$

In eqs. (10) and (11), E_{RES} is the total renewable energy generated.

Environmental impact

In order to realize the actual benefits arising from H_2 as a green product and renewable resource, one should take into account potential applications and contributions. One obvious properties of any green products is zero emission greenhouse gasses (GHG) specially CO_2 which is true also for H_2. Of course, its contribution indirectly effects the CO_2 emission depending on which end H_2 is supposed to use. In order to have a sense of such effect, the research group has taken into account application in building sector via blending into natural gas network in order to reduce the consumption rate.

Blending into natural gas network

The carbon avoided from blending process is not straightforward since it is not correlated linearly with H_2 concentration. Hence, a sixth grade polynomial relation which is developed in Ref. [58] and reported in eq. (15) used to evaluate $CO_{2\ avoided}$ from blending.

$$CO_{2\ avoided} = 20\ f_{H2}^6 + 8.87 f_{H2}^5 - 11.7 f_{H2}^4 + 2 f_{H2}^3 - 16.4 f_{H2}^2 - 16.1 f_{H2}^1 \tag{12}$$

In eq. (15) f represents H_2 concentration in blending. As of today, Italy does not have any legislation to constrain allowable H_2 concentration in natural gas network [59]. Yet, based on available studies, the maximum concentration rate without additional network equipment that can deliver same amount of energy is 20% [60,61]. In order to calculate decarbonization rate, so called "energy over price" (EOP) ratio is needed as well. EOP indicates the excess energy flow rate from blending is needed to provide same energy burnt by natural gas formerly. Eq. (16) introduce a practical formula for such parameter [58]:

$$EOP = \frac{LC_{H2NG}}{LHV_{H2NG}} - \frac{LC_{NG}}{LHV_{NG}} \tag{13}$$

LC is the levelized cost (€/Nm^3) of mixture and NG.

Result and discussion

sCO_2 HP performance

The sizing of sCO_2 HP is carried out regarding the various thermal load requirement. In this case, the starting point is the gas cooler and the heat load. Thermal load changes based on different steam flow rates corresponding to SOEC. By fixing the size of the gas cooler, cooling load corresponding to the gas heater is evaluated consequently. The simulation is performed for 20, 50, 75 and 110 kg_{steam}/h. Such values are correlated to the available commercial models representing 65, 160, 250 and 350 kW_{el} with the same steam to H_2 ratio [62]. As reported in Table 5, the size of the hot sink (gas cooler) rises progressively by increasing steam flow rate. The maximum available discharged heat from AEC is also calculated. Such heat is used to recover the cold sink load corresponding to the size of the gas heater inside the heat pump. As suggested by the results, increasing the size of SOEC improves the thermal efficiency which indicates the recovered heat from Alkaline stack. However, there is an upper limit for heat recovery. The simulation results shows the maximum thermal efficiency is near 73%. By increasing the flow rate above 110 kg_{steam}/h available heat cannot meet the cooling load. For instance in case of 120 kg_{steam}/h, the cooling load is equal to 41.96 kW whilst the available heat for recovery is 38.5 which is not sufficient.

The main parameter to describe the energy performance of sCO_2 HP is COP which can be evaluated from the Carnot ideal cycle:

$$\eta_{carnot} = \frac{T_H}{T_H - T_C} \tag{14}$$

In which T_H and T_C are temperatures at gas cooler and gas heater in K, respectively. The actual COP however is derived

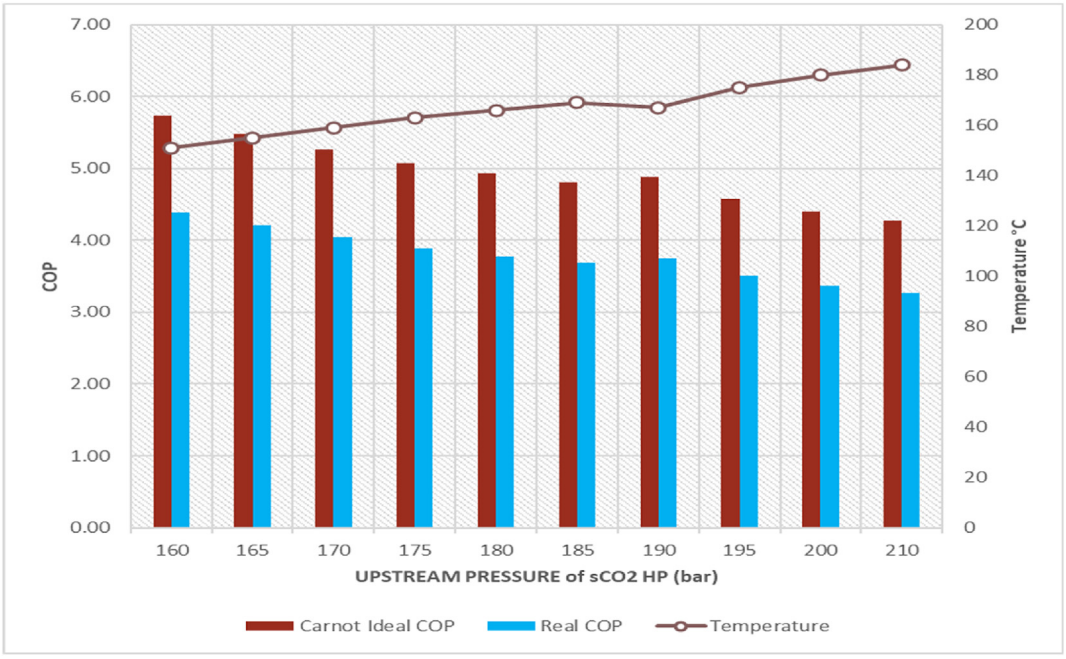

Fig. 4 – COP and temperature variation vs Upstream pressure.

considering the ratio between practical heat discharged and the imported work for compression:

$$\eta_{real} = \frac{Q_H}{W} \tag{15}$$

Fig. 4, shows the result of simulated ideal and real COP by changing the upper pressure. As illustrated, the upper pressure has reverse impact on the COP since it increases the work done by compressor. However, it results in higher available temperature in the gas cooler. Higher temperature is beneficial for the heat transfer process and sizing the gas cooler since the heat transfer is occur between two fluid in gaseous phase. The research group has decided to set the minimum temperature difference not below 30 °C in order to ensure the effective heat exchange between CO_2 and the water. As a result, T_H is kept at least 180 °C. having T and P as two effective parameters that constrain the performance of the heat pump, the optimum design point is set to 200 bar and 180 °C. In such condition the COP_{real} of the HP is equal to 3.25. The downstream pressure is set to 75 bar just slightly above critical point (73.81 bar at 31 °C). In this circumstance due to significant isentropic expansion inside expander, as explained in Methodology, the temperature profile of the refrigerant drops rapidly below the critical point which should be avoided. To address this issue, a mid-range pressure has been defined to ensure super critical condition. Taking a closer look at Fig. 4, a sudden increase in COP at 190 bar appears. Such a behaviour is correlated to the different mid-pressure from 185 bar so on.

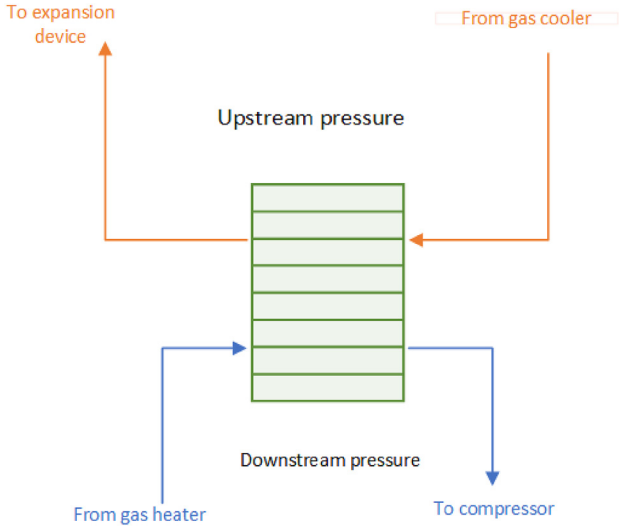

Fig. 5 – Input/output flows of internal heat exchanger.

Table 6 – The impact of mid-pressure to the output temperature and COP of the system.

Upstream pressure (Bar)	160	165	170	175	180	185	190	195	200	210
Mid- pressure (Bar)	100	100	100	100	100	100	120	120	120	120
Compression ratio (volve)	1.6	1.65	1.7	1.75	1.8	1.85	1.58	1.625	1.67	1.75
T_after expansion (°C)	36.49	35.38	34.34	33.36	32.43	31.56	36.02	35.10	34.22	32.59
COP Carnot	5.73	5.49	5.27	5.07	4.93	4.80	4.89	4.57	4.40	4.27
COP real	4.39	4.20	4.04	3.88	3.78	3.68	3.75	3.50	3.37	3.27
T_Gas cooler out (°C)	151	155	159	163	166	169	167	175	180	184

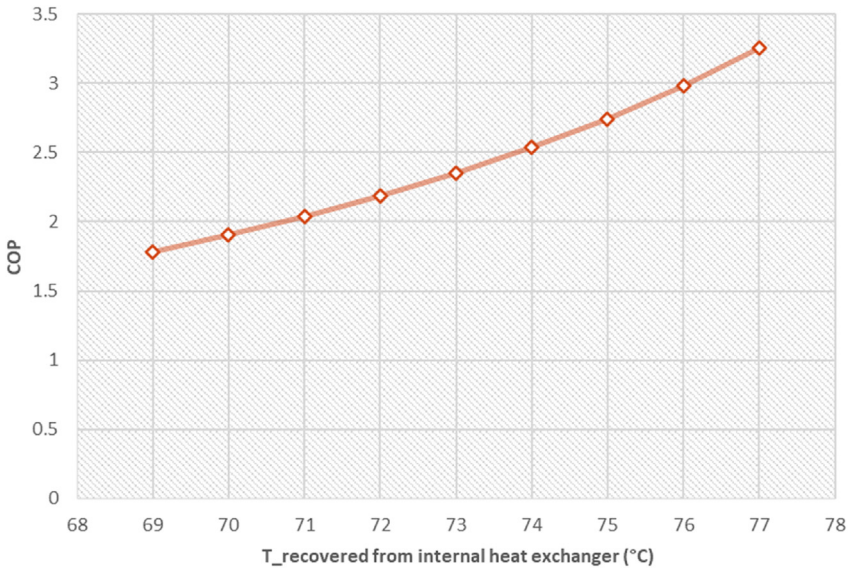

Fig. 6 – The impact of regeneration temperature to improve COP.

Starting from 160 bar as the high pressure value, up to 185 bar, the mid-pressure equal to 100 bar happens to be sufficient enough to fulfil the circumstances. The simulation results at 185 bar show temperature profile of the working fluid after expansion process is around 31 °C which is very close to the saturation temperature. By increasing the pressure from 185 to 190, the temperature falls below the critical point and the refrigerant condenses out. Eventually, from 185 to 190, a new mid-pressure is set from 100 to 120 bar. Such pressure is turned out to be sufficient up to 210 bar. Such a modification,

Table 7 – H_2 production results.

	20 $kg_{steam/h}$	50 $kg_{steam/h}$	70 $kg_{steam/h}$	110 $kg_{steam/h}$	SOEC only
Total Production (Nm^3/h)	107.36	112.14	116.13	121.71	138.9
SOEC production (Nm^3/h)	17.4	43.5	62.25	95.7	138.9
AEC production (Nm^3/h)	89.96	68.64	50.88	26.01	0
SOEC size (kW_{el})	62.64	156.6	234.9	344.5	500
AEC size (kW_{el})	431.8	329.5	244.2	124.8	0

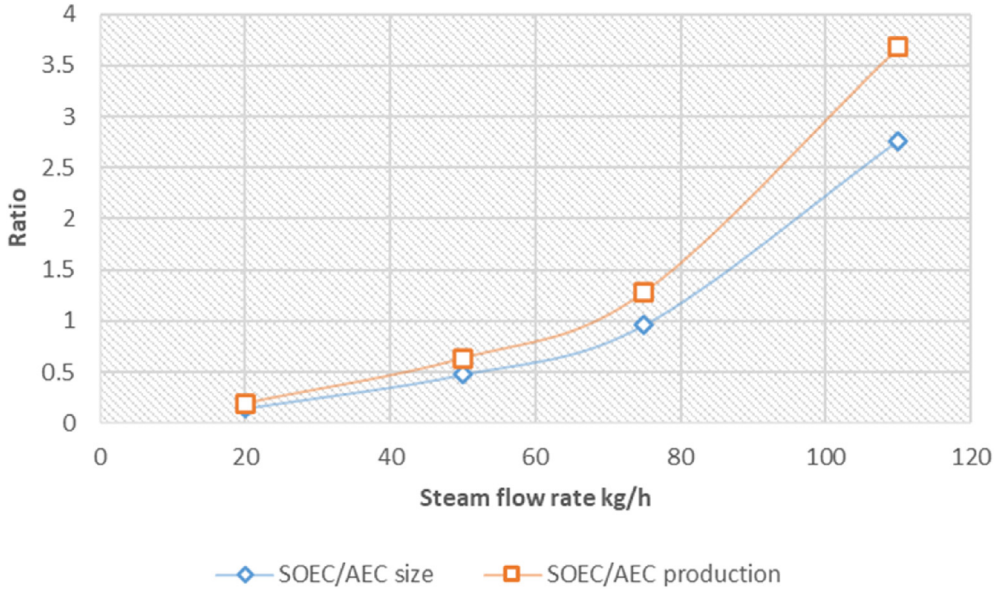

Fig. 7 – The difference between production and size ratio of SOEC/AEC.

Table 8 – Total energy efficiency report.

	0 $kg_{steam/h}$	20 $kg_{steam/h}$	50 $kg_{steam/h}$	70 $kg_{steam/h}$	110 $kg_{steam/h}$	SOEC only
EE	58%	60%	62%	65%	68%	65%

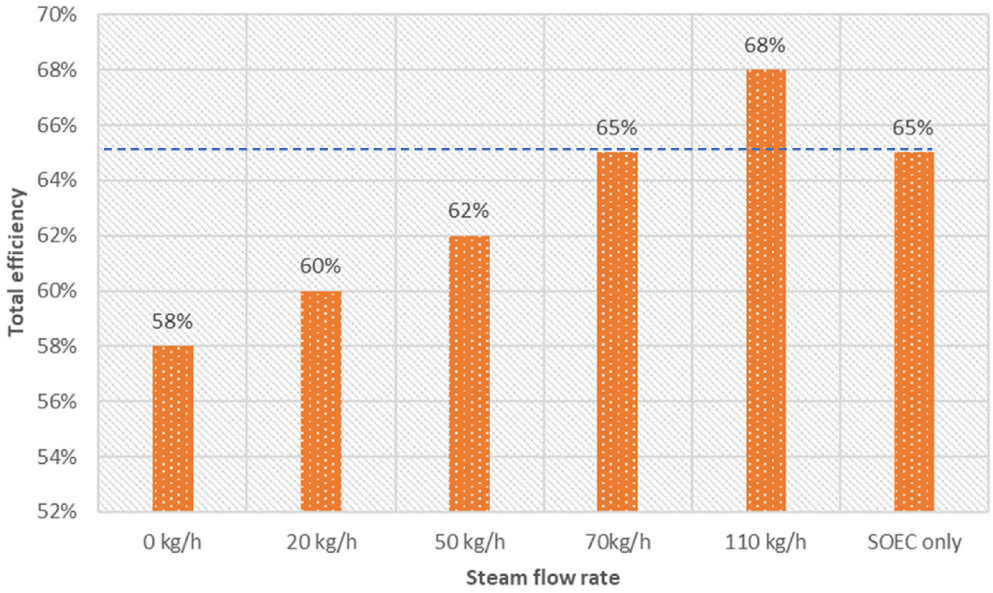

Fig. 8 – Total energy efficiency by changing the SOEC size.

changes the energy balance of the system specially after the gas heater. The eventual result suggest a slightly better COP performance at the cost of lower discharged temperature. Table 6, reports the simulation results that indicates the impact of mid-pressure on the key indicators of the heat pump.

Another effective parameter to improve the COP is related to the available heat to recover at internal heat exchanger. Such heat can be improved by increasing the heat exchanger effectiveness. Higher the effectiveness allows the effective heat transfer. Figs. 5 and 6, show the impact of internal heat exchanger design on the COP of the heat pump. The role of this heat exchanger is to recover the exhaust heat after gas cooling process. The simulation results shows the refrigerant after heating up the water in upstream cycle, and producing the steam at 150 °C, drops to 80 _85 °C. This temperature is still sufficient to heat up the downstream fluid which passes through the gas heater and has T around 55 °C. In this case, the isentropic compression starting point has higher temperature profile. The isentropic compression formula is brought in eq. (11), P_2 and T_2 are the output profile of the compressed fluid and P_1, T_1 describe the properties of the fluid before isentropic compression. κ is the ratio of C_p/C_v which is known as heat capacity. The left hand side of the equation is actually the thermodynamic work occurring inside the compressor. By increasing T_1, assuming the constant value for T_2, the work done by compressor reduces. As a consequence, the COP of the HP increases.

$$\left(\frac{P_2}{P_1}\right)^{\frac{k-1}{k}} = \frac{T_2}{T_1} \tag{16}$$

H_2 production

Table 7, shows the production rate corresponding to various SOEC-AEC contribution. The production rate increases progressively with the size of SOEC. This is due to the fact that SOEC offers more efficiency rather than AEC. However, such contribution is not correlated linearly with power consumption. As illustrated in Fig. 7, the production ratio between high and low temperature electrolysers is bigger than their power consumption. This gap become more wider as the size of SOEC enlarges. This is the technological superiority of SOEC which allows reaching higher H_2 production rate receiving the same amount of energy. Of course in the case of SOEC in solo mode, all the power is imported to SOEC unit and its production rate is the highest, but in this case an external heat source should provide thermal load since there is no heat available inside the system to recover.

Energy performance

From the method that is already introduced in Energy efficiency, the total energy of the system is derived. As the result suggested in Fig. 8, starting from 70 $kg_{steam/h}$, the total efficiency is as high enough as SOEC system alone. Of course, by increasing the flow rate the higher efficiency values are

reachable. These results are interesting since the coupling layout in general, presents lower electric efficiency than SOEC due to technical superiority of SOEC over AEC. However, thanks to heat recovery system and free available heat resource the total efficiency can increase. Considering AEC alone which represents 58% electric efficiency, coupling cases with any arbitrary flow rate offers higher efficiency. Such results are shown in Table 8 and Fig 8.

LCOH

Based on the financial assumptions that have been already introduced Economic assumption, the levelized cost of hydrogen in each scenario is calculated. It is noteworthy that such value is stack price before compression. At the moment, due to high initial cost of SOEC systems which is as high as 3000 €/kW_{el}, despite technological advances and energy

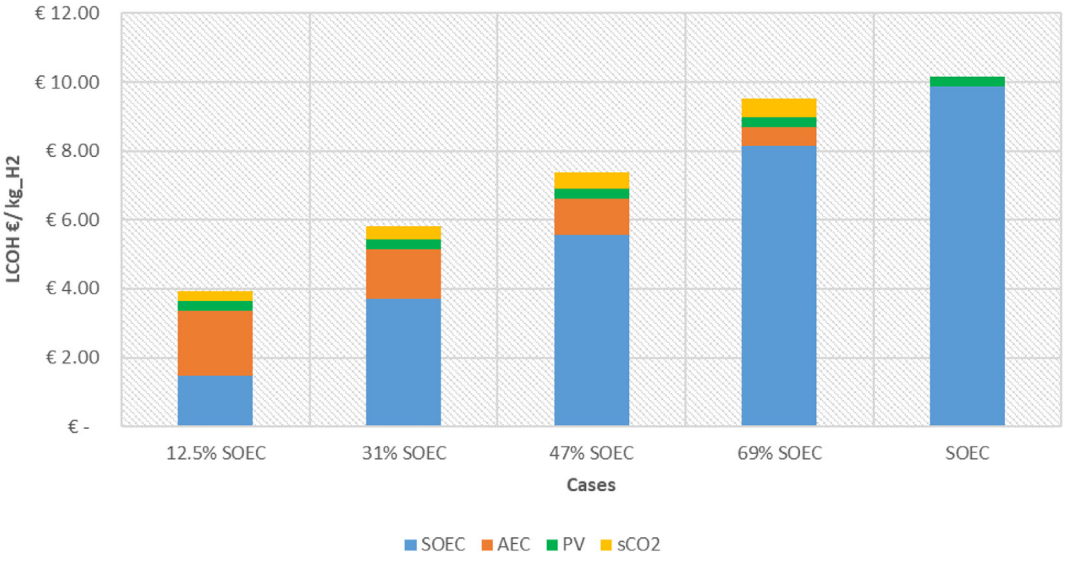

a. LCOH for each scenario supplied by PV

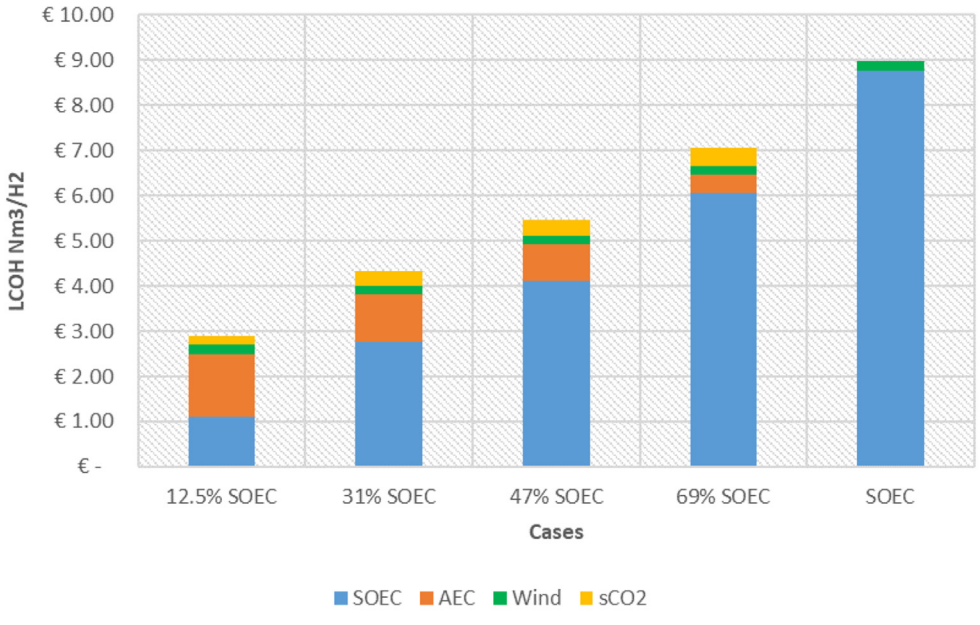

b. LCOH for each scenario supplied by wind

Fig. 9 – a)LCOH for each scenario supplied by PV. b)LCOH for each scenario supplied by wind.

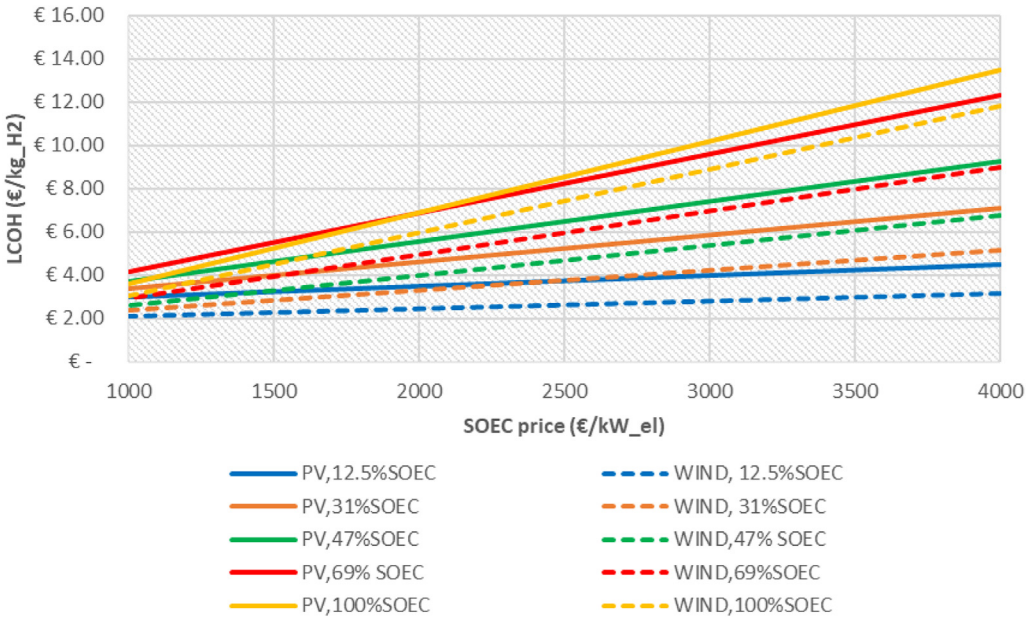

Fig. 10 – LCOH variation by SOEC price reduction.

indicators, it is considered as an expensive technology. However, it is expected by 2030 price falls below 1000 €/kW_{el}. Between PV and wind, the wind turbine has showed a better results due to higher capacity factor and lower LCOE for the region of Italy (see Fig. 9).

Sensitivity analysis

Fig. 10, shows the potential LCOH by decreasing the SOEC price. In comparison with low temperature electrolysis technologies, which offers currently LCOH in range of 3–4 €/kg_{H2}, SOEC in solo mode still will remain expensive. Unless the SOEC price drops below 2000 €/kW_{el}. Of course the impact of SOEC capex variation is more stronger for the cases with larger SOEC. For instance, in the case including wind and 12.5% of SOEC, the LCOH changes very slowly by large variation of SOEC price. In the contrary, in case including PV 100% SOEC, 300% reduction occurs in LCOH by changing SOEC capex from 4000 to 1000 €/kW_{el}.

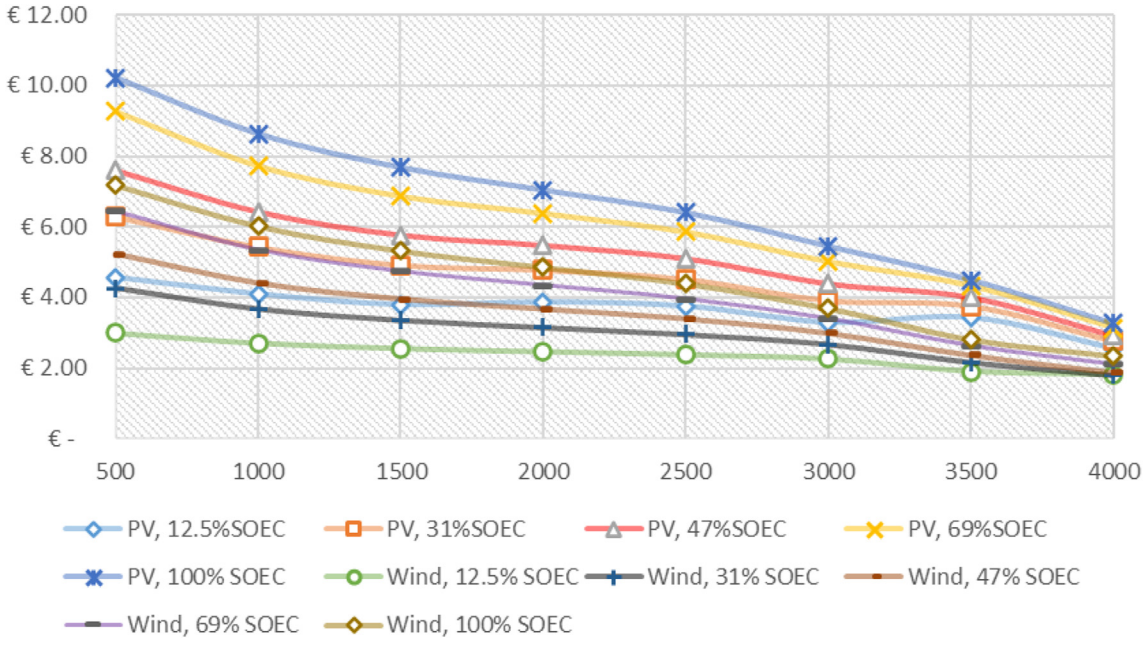

Fig. 11 – LCOH vs RES input.

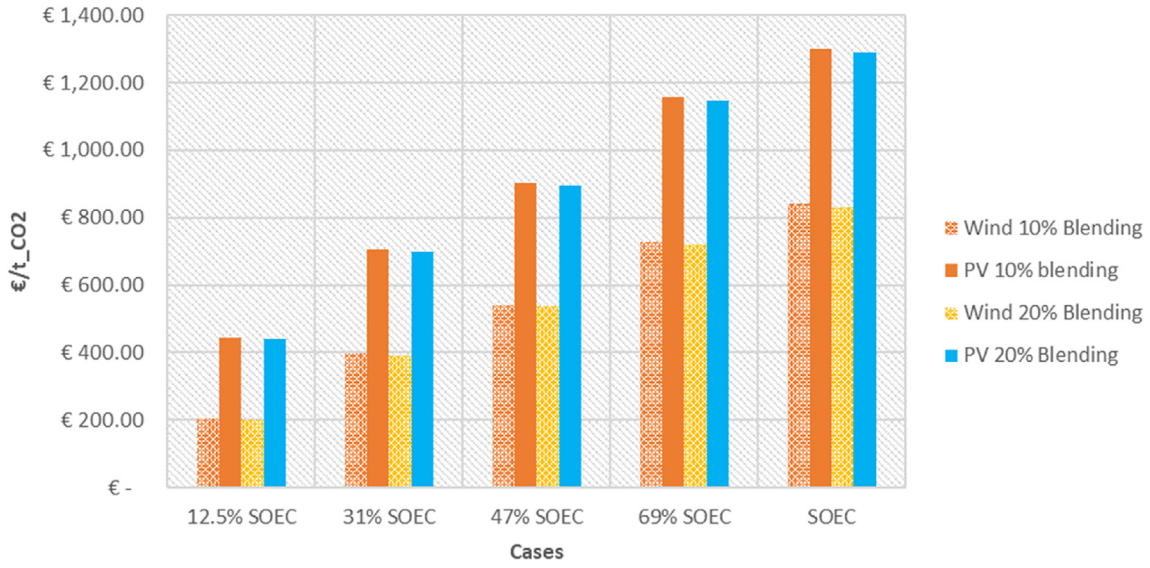

Fig. 12 – Decarbonization cost considering the blending into natural gas network.

Another sensitivity analysis is carried out considering different RES input. As explained before, based on the available commercial SOEC size, the renewable input has been fixed at 500 kW. Nevertheless, by assuming available SOEC commercial models with larger size in future, higher RES power plant can be established. In Fig. 11, the plants up to 4 MW RES are assumed. As the production rate increase, LCOH tend to fall down. LCOH below 4 €/kg_{H2} is reached for production rate more than 800 Nm^3/h. However, such reduction is directly correlated to the share fraction of SOEC. For cases composing smaller SOEC contribution, increasing the size of RES income is not altering LCOH significantly. However it can be concluded for the larger SOEC contributions, the size has more evident impact on final H_2 production results.

Carbon avoidance results

The blending H_2 into NG network causes less NG consumption and eventually less carbon emission rate. Such effect can be calculated following the methodology introduced in Blending into Natural gas network. H_2 can be produced in the pressure range of 30 bar right after injection from electrolyser. Such pressure is in the range of natural gas pipeline meaning that it could directly injected to the NG network without undergoing any further compression. As a result the final LCOH would be equal to the stack price which is already calculated. For blending into natural gas network, the values of 10 and 20% have been considered. The impact of recent energy crisis in Europe on the final price of NG has been taken into account. As reported in Ref. [63], the NG price for Italy is 0.117 €/kWh. The final results are shown in Fig. 12. There is a meaningful difference between PV and wind in the region of Italy. In average wind can cost around 40% less than PV for avoiding one ton of CO_2. The contribution of SOEC is directly correlated with EOP and eventually with decarbonization cost. As a result, rising the share of SOEC from RES, increase the price for saving a ton of CO_2. Such results can be observed in Table 9. In this case, the final results show very small dependency to blending variation.

Since renewable resource has been assumed for hydrogen production the electricity is also generated with zero carbon emission. In order to take into account also CO_2 saving from

Table 9 – Detailed results of decarbonization cost.

Cases	LCOH (€/Nm^3_{H2})	EOP(€/GJ)		Blending $CO_{2avoided}$ (€/t_{CO2})		Total $CO_{2avoided}$ (€/t_{CO2})	
		10%	20%	10%	20%	10%	20%
PV,12.5% SOEC	0.41	0.79	1.70	443.99	439.46	12.30	25.76
Wind, 12.5% SOEC	0.27	0.36	0.78	203.78	201.70	5.65	11.83
PV, 31% SOEC	0.57	1.25	2.70	705.23	698.04	19.54	40.92
Wind, 31% SOEC	0.38	0.70	1.52	396.21	396.17	10.98	22.99
PV, 47% SOEC	0.68	1.60	3.46	903.38	894.17	25.03	52.42
Wind, 47% SOEC	0.47	0.96	2.08	541.40	535.88	15.00	31.42
PV, 69% SOEC	0.83	2.05	4.44	1157.37	1145.57	32.07	67.16
Wind, 69% SOEC	0.58	1.29	2.79	726.78	719.37	20.14	42.17
PV, 100% SOEC	0.92	2.31	4.99	1301.23	1287.96	36.05	75.51
Wind, 100% SOEC	0.65	1.49	3.22	840.59	832.02	23.29	48.78

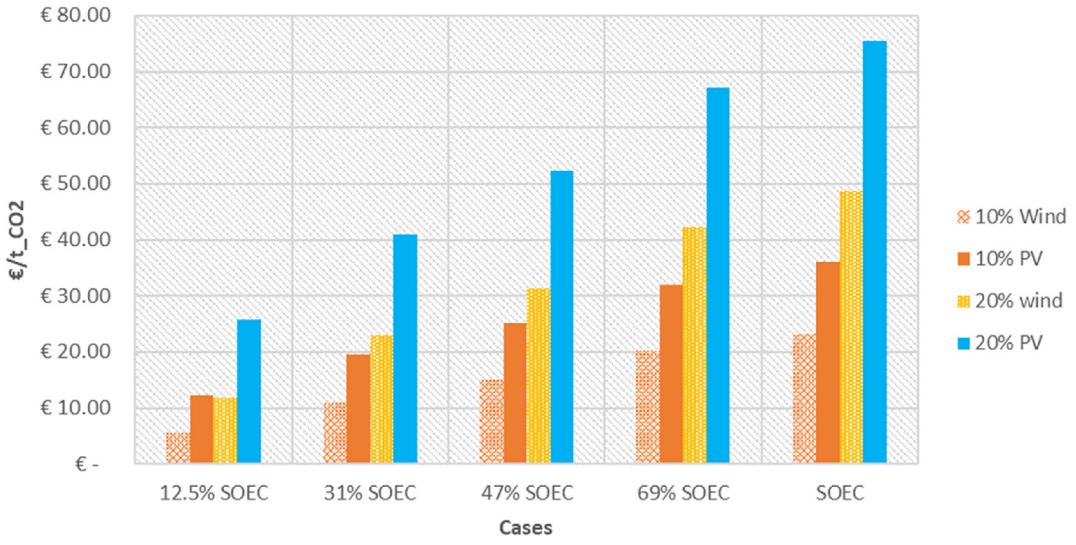

Fig. 13 – The total decarbonization cost considering the blending into natural gas network and electricity consumption.

the renewable resource, a total $CO_{2\ avoided}$ is introduced which is the saving from both blending and electricity consumption. As shown in Fig. 13, such consideration effects strongly the final results. Furthermore, the impact of blending percentage is more evident. The positive EOP values indicate the cost effectiveness of blending into natural gas which is due to the high LCOH at the moment to substitute NG network. However, in future if the LCOH falls behind the threshold value of 1.67 €/kg_{H2}, blending cost would be equal to NG capex. Below such value, negative EOP will be met indicating economic beneficial for decarbonization instead of excessive price.

Conclusion

This research study is conducted to justify the application of SOEC in commercial level. A layout composed of SOEC coupled with AEC through a heat pump is proposed. The heat pump system uses CO_2 operating in super critical state, recovering waste heat correlated with AEC and utilize it for steam generation. Such steam is corresponding to SOEC thermal input.

The simulation results proves technical superiority comparing with SOEC system in solo-mode. Some of the noteworthy outcomes are listed as follow.

1. Recovering up to 76% of thermal power that initially was exhausted by AEC.
2. COP equal to 3.25 for the sCO_2 HP for this application which can be improved even more by changing boundary conditions.
3. By assuming 500 kW RES, the production rate remains in the range of 107–138.9 Nm^3/h of H_2 based on different size of SOEC
4. The total efficiency of coupling system considering the thermal input can be even higher than SOEC in stand-alone mode. The results shows for SOEC/AEC size ratio equal or greater than 1.0, the total efficiency can be higher than SOEC.
5. LCOH varies in the range of 3–10 €/kg_{H2} in which wind offers cheaper prices.
6. Such results can be significantly improved by reducing technological cost of SOEC in near future or increasing the size of power plant. In this case, LCOH below 4 €/kg_{H2} is reachable.

Declaration of Competing Interest

The authors declare that they have no known competing financial interests or personal relationships that could have appeared to influence the work reported in this paper.

Nomenclature

CAPEX	Initial capital expenditures (€)
O&M	Operation and maintenance cost (€)
LCOE	Levelized cost of energy (€/kWh)
LCOH	Levelized cost of hydrogen (€/kg H_2)
LHV	Lower Heat Value (MJ/Nm^3)
COP	Coefficient of performance
EOP	Energy overprice (€/GJ)
EE	Energy efficiency
LC	Levelized cost of gas (€/Nm^3)
P	Pressure (Bar)
C	Heat capacity (J/kg.°C)
T	Temperature (.°C)
$\dot{m}$	Mas flow rate (kg/h)
m	Annual production (kg)
h	Enthalpy (KJ/kg)
Q	Thermal power (kW)
W	Thermodynamic work (kW)
E	Energy (kWh)
P'	Power (kW)
η	efficiency
κ	Isentropic compression
f	H_2 fraction in Natural gas blending
crf	Capital recovery factor
i	Annual interest rate
τ	Project lifetime (year)

Subscripts

el	Electric
th	Thermal
sat	saturation
sv	Saturated vapor
sl	Saturated liquid
w	water
dp	Design point
l	Losses
coupled	Low and high temp electolysers coupling scenario
H	Hot sink
C	Cold sink
d	Discharged
p	Constant pressure
v	Constant volume
regen	regeneration
tot	total

Abbreviations

AEC	Alkaline electrolysis
SOEC	Solid oxide electrolysis
PEM	Proton exchange membrane
sCO_2	Supercritical CO_2
GHG	Greenhouse gases
HTE	High temperature electrolysis
LTE	Low temperature electrolysis
WGS	Water Gas Shift
HP	Heat Pump
RES	Renewable energy source
PV	photovoltaic
NG	Natural gas
YSZ	yttria stabilized zirconia
PFSA	perflurosulfonated acid
LPG	Liquid pressurized gas
H_2NG	Hydrogen enriched natural gas

REFERENCES

[1] Acar C, Dincer I. Review and evaluation of hydrogen production options for better environment. J Clean Prod 2019;218:835–49. https://doi.org/10.1016/j.jclepro.2019.02.046.

[2] Abe JO, Popoola API, Ajenifuja E, Popoola OM. Hydrogen energy, economy and storage: review and recommendation. Int J Hydrogen Energy 2019;44:15072–86. https://doi.org/10.1016/j.ijhydene.2019.04.068.

[3] Pastore LM, Sforzini M, Lo Basso G, de Santoli L. H2NG environmental-energy-economic effects in hybrid energy systems for building refurbishment in future National Power to Gas scenarios. Int J Hydrogen Energy 2022;47:11289–301. https://doi.org/10.1016/j.ijhydene.2021.11.154.

[4] Atilhan S, Park S, El-Halwagi MM, Atilhan M, Moore M, Nielsen RB. Green hydrogen as an alternative fuel for the shipping industry. Curr Opin Chem Eng 2021;31:100668. https://doi.org/10.1016/j.coche.2020.100668.

[5] Nikolaidis P, Poullikkas A. A comparative overview of hydrogen production processes. Renew Sustain Energy Rev 2017;67:597–611. https://doi.org/10.1016/J.RSER.2016.09.044.

[6] Balat H, Kirtay E. Hydrogen from biomass – present scenario and future prospects. Int J Hydrogen Energy 2010;35:7416–26. https://doi.org/10.1016/J.IJHYDENE.2010.04.137.

[7] Liu S, Zhu J, Chen M, Xin W, Yang Z, Kong L. Hydrogen production via catalytic pyrolysis of biomass in a two-stage fixed bed reactor system. Int J Hydrogen Energy 2014;39:13128–35. https://doi.org/10.1016/J.IJHYDENE.2014.06.158.

[8] Wang Z, He T, Qin J, Wu J, Li J, Zi Z, et al. Gasification of biomass with oxygen-enriched air in a pilot scale two-stage gasifier. Fuel 2015;150:386–93. https://doi.org/10.1016/J.FUEL.2015.02.056.

[9] Fremaux S, Beheshti SM, Ghassemi H, Shahsavan-Markadeh R. An experimental study on hydrogen-rich gas production via steam gasification of biomass in a research-scale fluidized bed. Energy Convers Manag 2015;91:427–32. https://doi.org/10.1016/J.ENCONMAN.2014.12.048.

[10] Rashid MM, Mesfer MK Al, Naseem H, Danish M. Hydrogen production by water electrolysis: a review of alkaline water electrolysis, PEM water electrolysis and high temperature water electrolysis. Int J Eng Adv Technol 2015:2249–8958.

[11] Yu F, Yu L, Mishra IK, Yu Y, Ren ZF, Zhou HQ. Recent developments in earth-abundant and non-noble electrocatalysts for water electrolysis. Mater Today Phys 2018;7:121–38. https://doi.org/10.1016/J.MTPHYS.2018.11.007.

[12] Grigoriev SA, Fateev VN, Bessarabov DG, Millet P. Current status, research trends, and challenges in water electrolysis science and technology. Int J Hydrogen Energy 2020;45:26036–58. https://doi.org/10.1016/j.ijhydene.2020.03.109.

[13] Sergi F, Guzzini A, Brunaccini G, Aloisio D, Bianchini A, Pellegrini M, et al. Data collection and management – product specifications. 2021. p. 1–64.

[14] Carmo M, Fritz DL, Mergel J, Stolten D. A comprehensive review on PEM water electrolysis. Int J Hydrogen Energy 2013;38:4901–34. https://doi.org/10.1016/j.ijhydene.2013.01.151.

[15] Shiva Kumar S, Lim H. An overview of water electrolysis technologies for green hydrogen production. Energy Rep 2022;8:13793–813. https://doi.org/10.1016/J.EGYR.2022.10.127.

[16] Jin Z, Wang L, Chen T, Liang J, Zhang Q, Peng W, et al. Transition metal/metal oxide interface (Ni-Mo-O/Ni4Mo) stabilized on N-doped carbon paper for enhanced hydrogen evolution reaction in alkaline conditions. Ind Eng Chem Res 2021;60:5145–50. https://doi.org/10.1021/ACS.IECR.1C00039/SUPPL_FILE/IE1C00039_SI_001.PDF.

[17] Yoon Y, Kim H, Kim SK, Kim JJ. Acid-durable, high-performance cobalt phosphide catalysts for hydrogen evolution in proton exchange membrane water electrolysis. Int J Energy Res 2021;45:16842–55. https://doi.org/10.1002/ER.6936.

[18] Brisse A, Schefold J, Zahid M. High temperature water electrolysis in solid oxide cells. Int J Hydrogen Energy 2008;33:5375–82. https://doi.org/10.1016/j.ijhydene.2008.07.120.

[19] Herring JS, O'Brien JE, Stoots CM, Hawkes GL, Hartvigsen JJ, Shahnam M. Progress in high-temperature electrolysis for hydrogen production using planar SOFC technology. Int J Hydrogen Energy 2007;32:440–50. https://doi.org/10.1016/j.ijhydene.2006.06.061.

[20] Moseley PT. Fuel cell systems explained, 93; 2001. https://doi.org/10.1016/s0378-7753(00)00571-1.

[21] Laguna-Bercero MA. Recent advances in high temperature electrolysis using solid oxide fuel cells: a review. J Power Sources 2012;203:4–16. https://doi.org/10.1016/j.jpowsour.2011.12.019.

[22] AlZahrani AA, Dincer I. Modeling and performance optimization of a solid oxide electrolysis system for

hydrogen production. Appl Energy 2018;225:471–85. https://doi.org/10.1016/j.apenergy.2018.04.124.
[23] Ridjan I, Mathiesen BV, Connolly D. Synthetic fuel production costs by means of solid oxide electrolysis cells. Energy 2014;76:104–13. https://doi.org/10.1016/j.energy.2014.04.002.
[24] Vincent I, Bessarabov D. Low cost hydrogen production by anion exchange membrane electrolysis: a review. Renew Sustain Energy Rev 2018;81:1690–704. https://doi.org/10.1016/j.rser.2017.05.258.
[25] Proost J. State-of-the art CAPEX data for water electrolysers, and their impact on renewable hydrogen price settings. Int J Hydrogen Energy 2019;44:4406–13. https://doi.org/10.1016/j.ijhydene.2018.07.164.
[26] Bhandari R, Shah RR. Hydrogen as energy carrier: techno-economic assessment of decentralized hydrogen production in Germany. Renew Energy 2021;177:915–31. https://doi.org/10.1016/j.renene.2021.05.149.
[27] de Santoli L, Paiolo R, Lo Basso G. Energy-environmental experimental campaign on a commercial CHP fueled with H2NG blends and oxygen enriched air hailing from on-site electrolysis. Energy 2020;195:116820. https://doi.org/10.1016/j.energy.2019.116820.
[28] Medina P, Santarelli M. Analysis of water transport in a high pressure PEM electrolyzer. Int J Hydrogen Energy 2010;35:5173–86. https://doi.org/10.1016/j.ijhydene.2010.02.130.
[29] Suermann M, Bensmann B, Hanke-Rauschenbach R. Degradation of proton exchange membrane (PEM) water electrolysis cells: looking beyond the cell voltage increase. J Electrochem Soc 2019;166:F645–52. https://doi.org/10.1149/2.1451910jes.
[30] Grigoriev SA, Kalinnikov AA, Millet P, Porembsky VI, Fateev VN. Mathematical modeling of high-pressure PEM water electrolysis. J Appl Electrochem 2010;40:921–32. https://doi.org/10.1007/s10800-009-0031-z.
[31] Barbir F. PEM electrolysis for production of hydrogen from renewable energy sources. Sol Energy 2005;78:661–9. https://doi.org/10.1016/j.solener.2004.09.003.
[32] Udagawa J, Aguiar P, Brandon NP. Hydrogen production through steam electrolysis: model-based dynamic behaviour of a cathode-supported intermediate temperature solid oxide electrolysis cell. J Power Sources 2008;180:46–55. https://doi.org/10.1016/j.jpowsour.2008.02.026.
[33] Moçoteguy P, Brisse A. A review and comprehensive analysis of degradation mechanisms of solid oxide electrolysis cells. Int J Hydrogen Energy 2013;38:15887–902. https://doi.org/10.1016/j.ijhydene.2013.09.045.
[34] O'Brien JE, Stoots CM, Herring JS, Lessing PA, Hartvigsen JJ, Elangovan S. Performance measurements of solid-oxide electrolysis cells for hydrogen production. J Fuel Cell Sci Technol 2005;2:156–63. https://doi.org/10.1115/1.1895946.
[35] Königshofer B, Höber M, Nusev G, Boškoski P, Hochenauer C, Subotić V. Accelerated degradation for solid oxide electrolysers: analysis and prediction of performance for varying operating environments. J Power Sources 2022;523:230982. https://doi.org/10.1016/j.jpowsour.2022.230982.
[36] Minetto S. Theoretical and experimental analysis of a CO2 heat pump for domestic hot water. Int J Refrig 2011;34:742–51. https://doi.org/10.1016/j.ijrefrig.2010.12.018.
[37] Lo Basso G, de Santoli L, Paiolo R, Losi C. The potential role of trans-critical CO2 heat pumps within a solar cooling system for building services: the hybridised system energy analysis by a dynamic simulation model. Renew Energy 2021;164:472–90. https://doi.org/10.1016/j.renene.2020.09.098.
[38] Xu J, Liu C, Sun E, Xie J, Li M, Yang Y, et al. Perspective of S–CO2 power cycles. Energy 2019;186:115831. https://doi.org/10.1016/j.energy.2019.07.161.
[39] Ahn Y, Bae SJ, Kim M, Cho SK, Baik S, Lee JI, et al. Review of supercritical CO2 power cycle technology and current status of research and development. Nucl Eng Technol 2015;47:647–61. https://doi.org/10.1016/j.net.2015.06.009.
[40] Johnson GA, McDowell MW. Supercritical CO2 cycle development at Pratt & Whitney Rocketdyne. In: Supercritical CO2 power symposium; 2011. Boulder, Colorado, May 24e25.
[41] Publications O. (12) United States patent ent for. 2015. p. 2.
[42] White MT, Bianchi G, Chai L, Tassou SA, Sayma AI. Review of supercritical CO2 technologies and systems for power generation. Appl Therm Eng 2021;185. https://doi.org/10.1016/j.applthermaleng.2020.116447.
[43] Neises T, Turchi C. A comparison of supercritical carbon dioxide power cycle configurations with an emphasis on CSP applications. Energy Proc 2014;49:1187–96. https://doi.org/10.1016/j.egypro.2014.03.128.
[44] Bae SJ, Ahn Y, Lee J, Lee JI. Various supercritical carbon dioxide cycle layouts study for molten carbonate fuel cell application. J Power Sources 2014;270:608–18. https://doi.org/10.1016/j.jpowsour.2014.07.121.
[45] Sánchez D, Muñoz De Escalona JM, Chacartegui R, Muñoz A, Sánchez T. A comparison between molten carbonate fuel cells based hybrid systems using air and supercritical carbon dioxide Brayton cycles with state of the art technology. J Power Sources 2011;196:4347–54. https://doi.org/10.1016/j.jpowsour.2010.09.091.
[46] Wang G, Li Y, Jiang T, Chen Z. Effect study of super-critical CO2 parameters on heat transfer performance of U-shaped double-pipe heat exchanger. Case Stud Therm Eng 2022;30:101762. https://doi.org/10.1016/J.CSITE.2022.101762.
[47] Mojtahed A, De Santoli L. Hybrid Hydrogen production: application of CO2heat pump for the high-temperature water electrolysis process. J Phys Conf Ser 2022;2385. https://doi.org/10.1088/1742-6596/2385/1/012053.
[48] Motylinski K, Wierzbicki M, Kupecki J, Jagielski S. Investigation of off-design characteristics of solid oxide electrolyser (SOE) operating in endothermic conditions. Renew Energy 2021;170:277–85. https://doi.org/10.1016/j.renene.2021.01.097.
[49] Navasa M, Yuan J, Sundén B. Computational fluid dynamics approach for performance evaluation of a solid oxide electrolysis cell for hydrogen production. Appl Energy 2015;137:867–76. https://doi.org/10.1016/j.apenergy.2014.04.104.
[50] Prina MG, Manzolini G, Moser D, Vaccaro R, Sparber W. Multi-objective optimization model EPLANopt for energy transition analysis and comparison with climate-change scenarios. Energies 2020;13:1–22. https://doi.org/10.3390/en13123255.
[51] PVWatts Calculator. https://pvwatts.nrel.gov/pvwatts.php. [Accessed 25 February 2023].
[52] Ram M, Child M, Aghahosseini A, Bogdanov D, Lohrmann A, Breyer C. A comparative analysis of electricity generation costs from renewable, fossil fuel and nuclear sources in G20 countries for the period 2015-2030. J Clean Prod 2018;199:687–704. https://doi.org/10.1016/j.jclepro.2018.07.159.
[53] Ueckerdt F, Hirth L, Luderer G, Edenhofer O. System LCOE: what are the costs of variable renewables? Energy 2013;63:61–75. https://doi.org/10.1016/j.energy.2013.10.072.
[54] IREA. Renewable power generation costs in 2020. 2020.
[55] IEA. The Future of Hydrogen: seizing today's opportunities. Propos Doc Japanese Pres G20; 2019. p. 203.

[56] Global natural gas prices. https://www.globalpetrolprices.com/Italy/natural_g.
[57] Dai B, Qi H, Liu S, Zhong Z, Li H, Song M, et al. Environmental and economical analyses of transcritical CO2 heat pump combined with direct dedicated mechanical subcooling (DMS) for space heating in China. Energy Convers Manag 2019;198. https://doi.org/10.1016/j.enconman.2019.01.119. 0–1.
[58] De Santoli L, Lo Basso G, Bruschi D. A small scale H2NG production plant in Italy: techno-economic feasibility analysis and costs associated with carbon avoidance. Int J Hydrogen Energy 2014;39:6497–517. https://doi.org/10.1016/j.ijhydene.2014.02.003.
[59] Pastore LM, Lo Basso G, Livio de Santoli MS. Technical, economic and environmental issues related to electrolysers capacity targets according to the Italian Hydrogen Strategy: a critical analysis. Renew Sustain Energy Rev 2022;166:112685. https://doi.org/10.1016/j.rser.2022.112685.
[60] Quarton CJ, Samsatli S. Power-to-gas for injection into the gas grid: what can we learn from real-life projects, economic assessments and systems modelling? Renew Sustain Energy Rev 2018;98:302–16. https://doi.org/10.1016/j.rser.2020.110192.
[61] Jaworski J, Blacharski T. Study of the E ff ect of addition of hydrogen to. 2020.
[62] VTT Technical Research Centre of Finland Ltd. Review of electrolysis technologies and their integration alternatives. 2018. 35.
[63] Natural gas prices around the world. June 2022. GlobalPetrolPrices.com n.d. https://www.globalpetrolprices.com/Italy/natural_gas_prices/[Accessed 4 March 2023].